AIP | Biomicrofluidics
Fundamentals, Perspectives & Applications

#1 ORIGINAL RESEARCH JOURNAL IN THE FLUID AND PLASMA PHYSICS CATEGORY

Development of a three-dimensional cell culture system based on microfluidics for nuclear magnetic resonance and optical monitoring

Vicent Esteve, Javier Berganzo, Rosa Monge, M. Carmen Martínez-Bisbal, Rosa Villa, Bernardo Celda, and Luis Fernandez

Citation: Biomicrofluidics **8**, 064105 (2014); doi: 10.1063/1.4902002

View online: http://dx.doi.org/10.1063/1.4902002

View Table of Contents: http://scitation.aip.org/content/aip/journal/bmf/8/6?ver=pdfcov

Published by the AIP Publishing

Development of a three-dimensional cell culture system based on microfluidics for nuclear magnetic resonance and optical monitoring

Vicent Esteve,[1,2,a)] Javier Berganzo,[3] Rosa Monge,[1,4,5] M. Carmen Martínez-Bisbal,[2,6] Rosa Villa,[1,7] Bernardo Celda,[1,2] and Luis Fernandez[1,4,5]

[1]*Networking Research Center on Bioengineering, Biomaterials and Nanomedicine (CIBER-BBN), Valencia, Spain*
[2]*Department of Physical Chemistry, University of Valencia, Valencia, Spain*
[3]*Ikerlan, Gipuzkoa, Donostia, Spain*
[4]*Group of Structural Mechanics and Materials Modelling (GEMM), Aragón Institute of Engineering Research (I3A), University of Zaragoza, Zaragoza, Spain*
[5]*Aragon Institute of Biomedical Research, Zaragoza, Spain*
[6]*Center of Molecular Recognition and Technologic Development (IDM), Polytechnic University of Valencia—University of Valencia, Valencia, Spain*
[7]*Microelectronics Institute of Barcelona, National Center of Microelectronics, CSIC, Barcelona, Spain*

(Received 14 August 2014; accepted 4 November 2014; published online 18 November 2014)

A new microfluidic cell culture device compatible with real-time nuclear magnetic resonance (NMR) is presented here. The intended application is the long-term monitoring of 3D cell cultures by several techniques. The system has been designed to fit inside commercially available NMR equipment to obtain maximum readout resolution when working with small samples. Moreover, the microfluidic device integrates a fibre-optic-based sensor to monitor parameters such as oxygen, pH, or temperature during NMR monitoring, and it also allows the use of optical microscopy techniques such as confocal fluorescence microscopy. This manuscript reports the initial trials culturing neurospheres inside the microchamber of this device and the preliminary images and spatially localised spectra obtained by NMR. The images show the presence of a necrotic area in the interior of the neurospheres, as is frequently observed in histological preparations; this phenomenon appears whenever the distance between the cells and fresh nutrients impairs the diffusion of oxygen. Moreover, the spectra acquired in a volume of 8 nl inside the neurosphere show an accumulation of lactate and lipids, which are indicative of anoxic conditions. Additionally, a basis for general temperature control and monitoring and a graphical control software have been developed and are also described. The complete platform will allow biomedical assays of therapeutic agents to be performed in the early phases of therapeutic development. Thus, small quantities of drugs or advanced nanodevices may be studied long-term under simulated living conditions that mimic the flow and distribution of nutrients.
[http://dx.doi.org/10.1063/1.4902002]

INTRODUCTION

Nuclear magnetic resonance (NMR) is a technique that is widely employed in clinical practice for diagnosing and monitoring diseases in patients, particularly, when soft tissues are involved.

There are several modalities that exploit the different characteristics of this technique. For example, magnetic resonance imaging (MRI) produces high quality images of the inside of the human body that enable the precise localisation of alterations, whereas magnetic resonance

[a)]Author to whom correspondence should be addressed. Electronic mail: Vicent.Esteve@uv.es.

spectroscopy (MRS) provides spectra that are of considerable importance for determining the diagnosis, evaluating the prognosis, and conducting the follow up of diseases that are difficult to manage such as brain tumours.[1]

The use of new therapeutic and contrast agents in humans is very restricted, and testing in experimental animals will always be limited.

A detailed microscopic analysis of the response and NMR characteristics of cellular systems *in vitro* can provide very relevant information for the interpretation of clinical MRI and MRS monitoring observations. Moreover, testing and fine-tuning of the quantification of some parameters are possible at higher resolutions. These measurements can afterwards serve as well-founded references.[2]

Furthermore, a multimodal image comparison that includes optical microscopy will provide complementary information, which is often indispensable in clinical practice.

One common approach is the direct study of biopsies taken from the tissue of interest, which can be very informative but frequently has severe limitations.[3,4] *In vitro* cell culture is a key methodology in biomedical studies, and there is a growing demand for detailed *in vitro* analyses.[5] Nevertheless, the lack of knowledge about the functioning of living tissues and about the factors that induce and maintain the differentiation observed in several types of tissues, in particular, the heterogeneous phenotypes that tumoural cells show *in vivo*, limit their replication in research studies.

On the other hand, biotechnological research has generated great interest in the development of new drug delivery systems to improve both the pharmacological and therapeutic properties of drugs. Drug delivery systems based on nanomaterials offer easier penetration in certain regions of the body due to their small size and simple surface modification.[6–8]

For example, gold nanoparticles conjugated with antibodies have proved to be useful for both selective imaging and the photothermal ablation of cancer cells.[9–11] Their importance as contrast agents for NMR or as therapeutic agents relies on an understanding of their distribution, half-life and excretion from or storage inside the target cells, and the subsequent development of these cells and their neighbours.[12,13] Moreover, performing such a complete analysis requires long-term monitoring, including multimodal imaging and NMR, and the observation of an identical system (not a similar one reproduced in another plate) and each individual cell within that system.

To mimic the same conditions experienced by cells *in vivo* and to have maximum control of that environment, an active study in the scientific community is being conducted to develop devices that combine microfluidic and microfabrication techniques to construct structures and matrices that simulate the cellular environment inside living tissues.[14] Thus, the nutrients and signalling factors as well as the gas exchange and mechanical forces that the cells experience would be extensively controlled.[15–18]

The increasing sophistication of the lithography techniques and computer-directed construction used in the fabrication of chips and electronic devices allows the design of complex systems, in which several types of sensors can be integrated to implement "micro-scale laboratories" (Lab-on-a-Chip). Diverse materials are employed in the construction of such devices, but resins and polymers [PDMS (Polydimethylsiloxane), COP (Cyclo Olefin Polymers), PMMA (Poly(methyl methacrylate)), SU-8, etc.] are predominately used. A wide variety of designs for specific applications are being developed, although most of these designs are still at a preliminary stage of development.[19]

NMR microscopy has developed in parallel with the standard macroscopic image techniques used in clinical and animal applications.[20–22] However, further developments and applications will require increased resolution and adequate methods for handling small living samples. Such technological challenges can only be addressed by a close and coordinated collaboration with specialised developers.

Several home-made devices for containing cells during NMR analysis have been prepared for specific studies. Some of these are designed for bulk spectroscopy[23] and others are designed for microimaging[24] or a combination of microimaging and spectroscopy,[25,26] and some are also designed to include fluidics.[23] However, none of these devices are easy to use with standard commercially available equipment, and in general, they are of limited scope.

Here, we describe a new device capable of long-term monitoring of organotypic cell cultures by NMR and optical techniques. The aim was to develop a complete platform that permits a multimodal analysis of a 3D cell culture, while maintaining conditions that mimic natural tissue, including the flow of nutrients and the cellular microenvironment. Our results report the development of a microfluidic chip for cells based on SU-8 as well as its packaging for easy handling, replacement, and coupling to NMR electronics. We present a preliminary NMR analysis of neurosphere cultures to show the potential feasibility of the device.

NEW MICROFLUIDIC DEVICE DESIGN

While there are already many different approaches to obtaining stable cell cultures on microfluidic devices, coupling such devices to an NMR system for monitoring remains challenging in practice. As a result, these devices suffer from limitations in sensitivity and resolution. The strategy selected in this design aims to increase the signal-to-noise ratio using a microcoil in close proximity to the sample and to obtain maximum resolution using strong magnetic gradients. As the microfluidic chip is intended to be disposable, the microcoil is fabricated with a different substrate, and is then placed directly on top of the cell microchamber by using a dedicated packaging (see Figure 1). Moreover, to achieve a minimal distance between the microcoil and the biological sample under study, a thin layer is used for the fabrication of the microchamber cover (75 μm). The total thickness of the chip is 550 μm. This allows for insertion into the microgradient device while maintaining optimal proximity to the magnetic fields (Figure 1(d)).

The complete assembly of the microfluidic device was designed to include the following items:

(a) A PCB (Printed Circuit Board) with an integrated microcoil fabricated by Bruker Biospin (Karlsruhe, Germany) and now commercially available with several microcoil diameters (Coil-on-a-chip Technology, product code: PI610M50).

(b) A microfluidic chip for cell culture (see detail of the design in Figure 2) that is designed as follows: Microfluidic devices were fabricated using SU-8 photolithography combined with an SU-8 to SU-8 bonding process.[27,28] SU-8 is an NMR-compatible material that offers high fabrication resolution,[29] transparency for optical inspection,[30] enough mechanical stability for easy handling and coupling with the microcoil,[31,32] and biocompatibility for use as a structural material for cell culture applications.[33–37] The final design of the device is presented in Figure 2 and consists of a 56 mm long chip that includes a 2 by 2 mm microchamber. The microchamber can be reached through four dedicated microchannels, which allow the required microfluidic control and facilitate access to the optical sensors. Each one of these four microchannels has a dedicated task as follows:

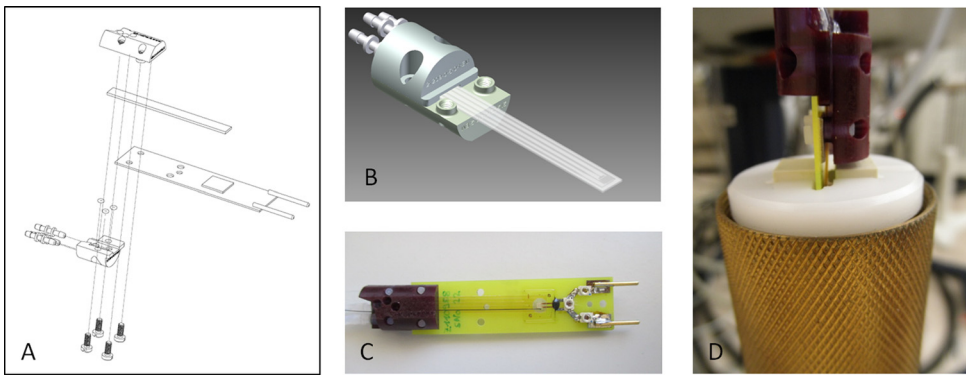

FIG. 1. (a) View of the device parts assembly. (b) Cell culture chip packaged with microfluidic connections. (c) The PCB is screwed to the packaging to place the microcoil in close contact with the cell culture microchamber. (d) The system is mounted inside the NMR sensor.

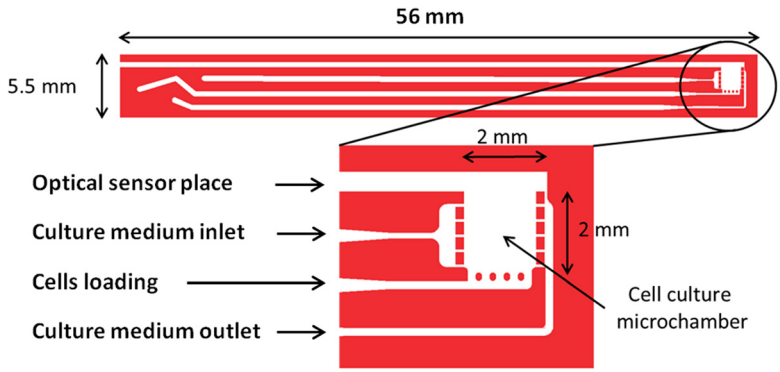

FIG. 2. Top view of the microfluidic chip design showing the most relevant features and dimensions.

Optical sensor placement: This microchannel holds the optical fibres used as sensors. The fibre is introduced through the microchannel until the tip finds the main culture chamber. Readout from the fibre is then used for temperature and pH monitoring.

Nutrient inlet: This microchannel is used for the perfusion of nutrients to the microchamber. A constant flow is applied to refresh the oxygen and nutrient concentration during the cell culture experiment. Low-flow rates ($<1\ \mu$l/min) were applied to avoid a dragging effect on cells under culture, which could result in voiding the microchamber.

Cell loading: Cells are carried through this microchannel to fill the microchamber. To allow the use of cell aggregates (like neurospheres) and to avoid clogging, the channel width is at least 200 μm or wider.

Nutrient outlet: Nutrients and waste residuals exit the chamber using this microchannel. As shown in Figure 2, pillars have narrow distances between them (75 μm) to prevent cell aggregates from being dragged out of the microchamber.

(c) A packaging body that supports the fluidic connections as well as the whole assembly by dedicated screws and joints (see Figure 1) that is designed as follows: The package is divided into two parts: a micro-device holder and an upper cover. The micro-device holder lodges the inlet-sealing o-rings and connects them to three fluidic tube connectors by means of internal channels. It also has mechanical clamps to fix the package to the NMR sensor. As long as the cover is screwed down over the chip holder, the micro-device is sealed and coupled to the tubes and is mechanically attached to the NMR sensor.

MATERIALS AND METHODS

Fabrication

The fabrication of the microfluidic device starts with the temporary bonding of a Kapton™ film on top of a 4″ Pyrex™ wafer. Kapton is used because it has low adhesion to SU-8, enabling an easy final release of the device once the fabrication has concluded. Then, an 80 μm thick SU-8 layer is spun and soft-baked (SB) by heating the wafer in two steps; first up to 65 °C for 10 min and then up to 95 °C for 30 min. Once the SB treatment finishes, an exposure of 400 mJ cm^{-2} is performed using a mask, which will define the bottom layer of the microfluidic channel. Next, a post-baked (PB) treatment is applied by heating the wafer up to 65 °C for 5 min followed by 95 °C for 15 min. Then, a 160 μm thick SU-8 layer is processed on top by repeating the process described above twice, using the same SB, exposure, and PB steps. The exposure step is performed using the same parameters, while using a new mask, and in this case, the mask defines the microchannels and chambers. Then, a 20 μm thick layer is processed for use as a bonding layer. While the SB parameters are kept the same, the PB parameters are changed by reducing the heating step at 95 °C down to 7 min. Then, using another 4″ Pyrex wafer with a Kapton film laminated on top, a new 80 μm thick layer of SU-8 is processed as previously described to define the cover of the microchannels. This layer includes holes for use as

fluidic inlets and outlets. Then, two 80 μm and one final 20 μm thick SU-8 layers are processed on top using the same mask used in the first wafer to define the microchannels but reversed. Finally, both wafers are aligned and bonded by applying a pressure of 3 bars at a temperature of 100 °C. Finally, the devices are manually released.

To avoid interferences in the measurement process, no conducting or magnetic materials are used for any part of the package. The micro-device holder and the cover are made of an epoxy resin and are fabricated by stereolithography. This technology allows each part to be built in a very compact and accurate way, including screws, internal channels of any shape, alignment features, etc. The sealing o-rings are made of a silicone elastomer, the fluidic connectors are made of PEEK, and the screws are made of nylon.

Assembly

Optical fibre-based sensors of pH (PRESENS™, pH-1Micro) and temperature (LumaSense™, Fluoroptic Temperature Probe) are introduced into the microchamber and sealed (Figure 3(c)).

The whole device is assembled on the packaging holding the microfluidics and fastened by dedicated plastic screws. Thus, the device can be inserted together with the PCB containing the coil inside the magnetic gradient system for NMR analysis, or it can be mounted on a base for optical monitoring during the culture.

A supporting base with an integrated design made of methacrylate that allows for the replacement of parts has been developed to prepare and monitor the system when it is outside the NMR equipment. The support incorporates a Peltier plate for thermostatting and several parts to hold and protect the chip and to encapsulate the fluidics and fibre optics. A microcontroller directs the thermostatisation and mechanical operations. We have incorporated a camera for time-lapse recording of the microchamber contents.

Finally, a mini-cabin has been constructed to protect and isolate the monitoring system from physical damage, dust, and thermal fluctuations. The assembly parts are made of methacrylate and aluminium and permit access from all sides. A wide frontal sliding shutter allows the supporting base to be placed inside the cabin and manipulated from within the cabin. Two

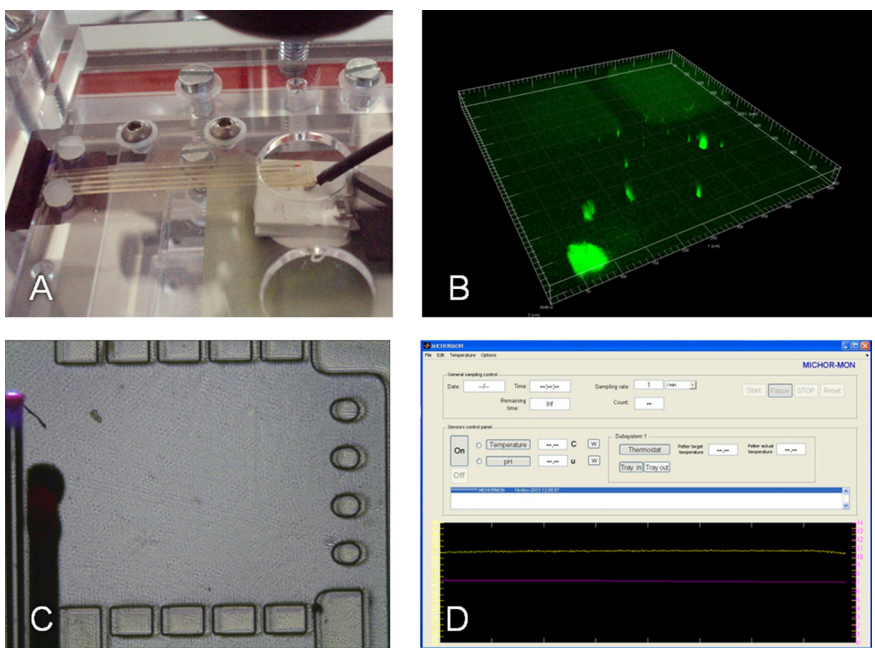

FIG. 3. Monitoring and control. (a) View of the device mounted on the monitoring base. (b) Confocal 3D image in which the background fluorescence emitted by the SU-8 can be observed; the shape of some pillars are visible at the top, while inside the main chamber, only some silica-based particles containing fluorescence are clearly visible with little background intensity. (c) View of the main culture microchamber where the tips of the fibre optic sensors are visible on the left of the image. (d) Window presenting the GUI of the control and visualisation software MICHORMON.

lateral and two rear windows also provided with sliding shutters allow the insertion of conductions and cables for external connections. The cabin can be mounted over a basic damping platform or optical board of metric spacing (more information available upon request).

The background fluorescence and resolution obtainable by multiphoton fluorescence microscopy were tested, proving the feasibility of the system (plastics often emit some fluorescence, but in this case, the thin cover used emits a low amount of background fluorescence around the culture chamber, see Figure 3(b) for a bi-photon confocal microscopy assay on an Olympus™ FV1000MPE microscope). Home-made software was developed in Matlab to control the whole system (temperature, sensor activation, data logging, etc.; see Figure 3(d)).

Neurosphere culture

Neurospheres were grown using a bank of stored precursor cells obtained from the subventricular zone of rat brains prepared in previous experiments.[38] The cells were dispersed mechanically and cultured for 7 days in Petri dishes with Dulbecco's modified Eagle's medium DMEM:F12 containing 10% FBS (fetal bovine serum) at 37 °C with an air atmosphere containing 5% CO_2 until neurospheres of a mean diameter of approximately 300 μm were formed. The medium was supplemented with an N2 hormone mix and EGF (epidermal growth factor) and bFGF (basic fibroblast growth factor) as mitogens.[39] The neurospheres were introduced into the microchamber by injection through the dedicated loading channel of the microfluidic device. The system was maintained at 37 °C, and the basal DMEM:F12 medium with 10% FBS was provided at a low-flow rate of 10 nl/min if not otherwise specified.

NMR

NMR microscopy and spectroscopy were carried out in a Bruker™ spectrometer at 14 T with 60 A xyz gradient amplifiers (GREAT 60) using a Micro5 probe and surface microcoils (500 μm internal diameter). Spatial gradients were generated with a new high-gradient system adapted to such microcoils (3000 G/cm).

Gradient echo-based image pulse sequences were tested using a 7–15 ms echo time, a 2 mm field of view, 128–512 scans and a 1–4 h total acquisition time. The experiments generated a matrix of data points of 256×256 and 128×128.

Single-voxel localised spectra were acquired using a PRESS sequence with water suppression on a volume of 8 nl ($0.2 \times 0.2 \times 0.2$). The acquisition time was 1 h 42′ (4098 scans).

Tests of the flow control, of the microimage analysis of the injection system, and of the fluid dynamics were performed by Gradient Echo and MDEFT (Modified Driven-Equilibrium Fourier Transform) pulse sequences using flows of 0, 0.2, 1, 10, 100, and 500 μl/min. Data were acquired as a matrix of 64×64 using four scans.

RESULTS AND DISCUSSION

Microfluidic device

The resulting SU-8-based microfluidic device is shown in Figures 1 and 3(a). As can be observed, no curvature is obtained despite the unusual length of the chip and the high internal stress associated with SU-8 fabrication processes. As a result, a good contact between the cell culture microchamber and the microcoil can be achieved, resulting in a higher NMR analysis resolution. The planarity of the chip was obtained, thanks to the fabrication process strategy, which was based on the bonding of two similarly structured SU-8 films. Being equal in thickness and exactly mirrored in design when finally bonded, the SU-8 chip deflection is negligible. This is because internal stresses from both SU-8 layers work in opposite directions, resulting in a planar device. Moreover, the fabrication process facilitates the safe development of the required micropillars. If such structures had been fabricated on the same SU-8 layer, it would have been difficult to ensure complete SU-8 development without a high risk of pillar tilting or even complete detachment.

This microchamber was designed to fit the new microgradient devices used in Bruker equipment to obtain maximum resolution when working with small samples. In particular, the

necessary proximity to the surface of the new planar microcoil required a very thin (approximately 75 μm) cover surface over the growth chamber area. This design allows the exploitation of the capabilities of the microcoils and microgradients, while the cell culture is maintained independent of the electronic system.

A long free surface of the chip outside the encapsulate is required for insertion into the NMR equipment and for reaching the microcoil position, but this makes the chip very susceptible to damage and bending. This problem requires construction of a dedicated holding system to enable the chip to function outside of NMR devices. The holding system is composed of a cabin and a basement that can support the attachment of the thermal control and the optical monitoring devices.

The size of the pre-chamber was adjusted to guarantee a uniform flow entering the main microchamber. Despite the reduced thickness of the chip, it supports fast flows of approximately 1 ml/min, which can be useful for cleaning and bubble elimination during the preparation of the chamber prior to receiving cells. The size of the microchamber (approximately four square millimetres) requires small quantities of cells and medium, thus an organotypic piece of tissue up to a maximum 400 μm thickness can be readily obtained. A dedicated microchannel allows the cells to be placed directly inside the main culture chamber, while the medium flow continues through the pre-chamber, thus circumventing any clogging created during the injection of cells. This offers a major degree of manoeuvrability.

Cell culture

Neurospheres of approximately 300 μm diameter were injected into the microchamber and were successfully grown for 48 h until coalescence. Then, we eliminated the mitogens from the medium (EGF and bFGF growth factors), allowing cells to differentiate for 72 h. A variety of morphologies characteristic of neuronal and radial glia were obtained, including the formation of a 3D structure (see Figures 4(a) and 4(b)). A low flow of approximately 10 nl/min was used to maintain a local microenvironment around the cells that allowed an adequate renovation of the medium.

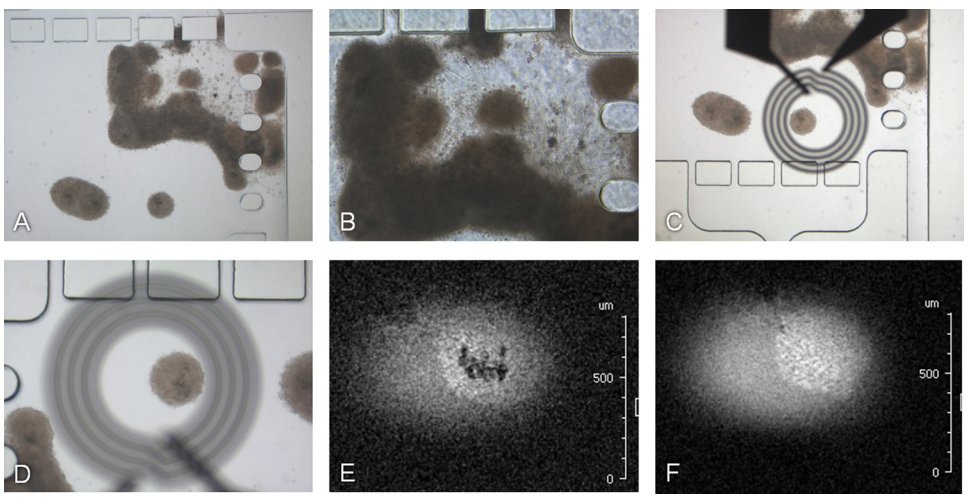

FIG. 4. Images of the neurospheres growing inside the microfluidic device. (a) Some neurospheres coalesced, growing in a corner at the entrance of the cell conduction channel. (b) The shape of the differentiated cells is indicated by a 3D outgrowth from the aggregated mass. (c) and (d) Optical images with the microcoil superimposed onto the microchamber and showing a neurosphere centred inside; (d) is inverted with respect to (c) to compare with the next images. (e) and (f) NMR microimages obtained at two different sections 180 μm apart; only the area covered by the microcoil appears "illuminated;" in (e), an internal and presumably necrotic area can be observed in this central section, whereas it is not visible in the most superficial section in (f). The in-plane resolution is 8×8 μm, whereas the slice thickness is 50 μm.

NMR analysis

NMR microimaging and localised spectroscopy techniques were adapted from our previous work studying brain tumour biopsies to optimise resolution on a standard base.[40]

We initially performed fluidic assays with NMR standard tubes and capillary tubes to test the performance of the main experiments at different flow rates of medium inside the NMR instrument, and the whole performance of the injectors was tested. Then, we conducted flow tests with the microfluidic device. The results showed no differences between the images obtained with stopped flow conditions and those obtained with a 0.2 μl/min flow. We observed a clear disruption when the flow was increased to over 100 μl/min.

When neurospheres were cultured inside the microchamber, we were able to obtain a preliminary set of images and spatially localised spectra. The images (see Figure 4) show a darkened area that is most likely due to the presence of a necrotic area in the interior of the neurospheres, which can frequently be observed in ordinary histological preparations when the distance to the surface impairs the diffusion of oxygen.

The spectra acquired in a volume of 8 nl inside the neurosphere show an accumulation of lactate that is indicative of anoxic conditions (Figure 5) and is something commonly found in the necrotic areas of glial tumours.[3] The signal-to-noise ratio for the lactate signal was 19 and was only 5 for the glucose signals. We currently are working to improve both the signal-to-noise ratio and resolution by adapting the standard pulse sequences to the new hardware. We are testing changes in the pulse sequences to speed-up the signal acquisition and increasing the sampling rate. We also will collaborate in new designs of the PCB implementation of the microcoils to improve the sensitivity and the extension of the field of view.

Control

Two optical fibre sensors allowed the temperature and pH to be monitored two times per minute inside the microchamber. Both sensors are based on the sensitivity of a specific fluorophore (quantifying variations produced in the emission spectra) to the changes in temperature and pH in the microenvironment.

Thermostatisation was realised using a Peltier plate and a microcontroller that stabilised the temperature to approximately 37 °C. Measurements at 12 h reported a standard deviation of approximately 0.1 for the temperature and pH (mean value of 7.2 for pH).

We developed a basic software platform for the concerted monitoring of the different fibre optic sensors, optical imaging, and thermostatisation. A graphical user interface allows selection of the data login, configuration of the sensors, targeting of the temperature control, and visualisation.

Though more complex designs for the culture microchamber could be helpful for specific applications, for example, to direct or control cellular growth, other alternatives are also

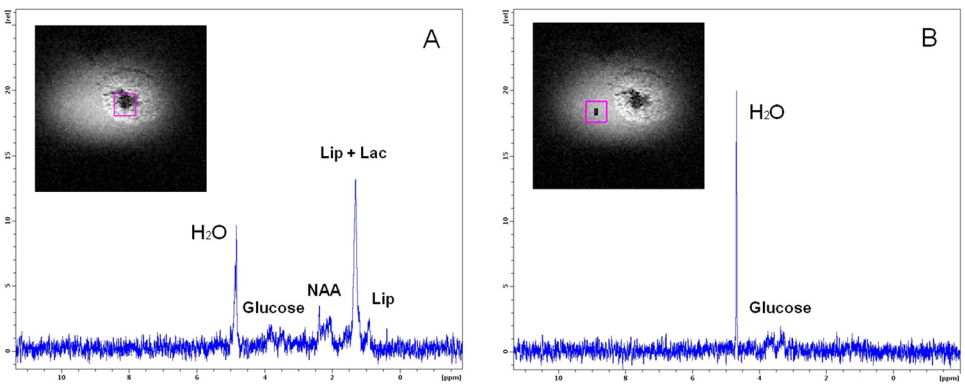

FIG. 5. NMR water-suppressed 1H spectra obtained inside (a) and outside (b) the neurosphere in a localised voxel of 8 nl. Some tentative designations are labelled in the figure. A considerable amount of lactate and lipids seem to be present in the necrotic interior.

possible. We have successfully inserted a specific scaffold during fabrication, which opens the possibility of developing and incorporating independently made pieces of scaffold with the required features to allow a broader array of applications.

CONCLUSIONS

Over the last few years, we developed a prototype micro-reactor (lab-on-chip) for the long-term monitoring of tissue samples and organotypic cellular systems with special characteristics that allows the use of NMR microscopy and/or optical techniques for molecular imaging. The system maintained 3D cellular cultures within an environment similar to the conditions of natural tissue, including the flow of nutrients and the cellular microenvironment. Moreover, specific tools were developed to control the system (integration of temperature sensor, pH sensor, Peltier plate, etc.).

Neurospheres were successfully seeded, grown, and differentiated inside the microfluidic chamber to generate a 3D cell culture network. The system allowed the monitoring of temperature and pH inside the microchamber. The images obtained using the system confirmed the presence of necrotic areas in the sections with less access to fresh nutrients, as observed in the histological analysis of real samples. Finally, spectra acquired by NMR in a volume of 8 nl inside the neurosphere showed an accumulation of lactate indicative of anoxic conditions, confirming the viability of NMR analysis within the microchamber.

The whole system constitutes a single platform that will allow several biomedical assays of therapeutic agents to be performed while also being monitored by NMR and optical techniques. The system will require small quantities of drugs or nanodevices, which will be able to reach the cells through a flow system that more closely approximates living conditions than plated cell cultures.

NMR is a non-invasive technique that provides structural and physiological information, which is a characteristic that we believe to be essential for monitoring a live cell assay with minimal disturbance. This micro-device could be of great help in the quest for new powerful clinically relevant image biomarkers directed to specific macromolecular targets while using minimal amounts of product.

Future developments will require a more advanced design for the cell culture platform to maintain real 3D tissue development, including special features from the natural microenvironment as well as the control of these features. To this end, we have initiated attempts to combine 3D scaffold technologies with the microsystem device prototype for organotypic cell culture. Three-dimensional scaffolds with different features at the macro, micro, and nano scales will be fabricated with rapid prototyping techniques alone or in combination with electrospinning.[41] These platforms will allow the precise control of the pore structure and architecture of the fabricated scaffolds, resulting in 3D matrices with controlled structural, physicochemical, and mechanical properties that can be elaborated independently and then inserted into the culture chamber.

ACKNOWLEDGMENTS

This work was supported partially by the Basque Government under the Etortek-Microsystems Programme, the ERANET-Neuron Project EPINet (EUI2009-04093) and SAF2009-14724-C02-02 from the Spanish Ministry of Science and Innovation and the European Regional Development Fund. The authors would like to thank Jorge Elizalde (Ikerlan S. Coop.) for their help and support and CIBER-BBN for general funding and support of the project.

We want to acknowledge Bruker Biospin for the kind collaboration which allowed the adaptation of their microcoils and our micro-reactor.

[1]A. Horská and P. B. Barker, "Imaging of brain tumors: MR spectroscopy and metabolic imaging," Neuroimaging Clin. N. Am. **20**(3), 293–310 (2010).
[2]C. Mountford, C. Lean, P. Malycha, and P. Russell, "Proton spectroscopy provides accurate pathology on biopsy and in vivo", J. Magn. Reson. Imaging **24**(3), 459–477 (2006).

[3]V. Esteve, B. Celda, and M. C. Martinez-Bisbal, "Use of 1H and 31P HRMAS to evaluate the relationship between quantitative alterations in metabolite concentrations and tissue features in human brain tumour biopsies," Anal. Bioanal. Chem. **403**(9), 2611–2625 (2012).
[4]V. Esteve, B. Martinez-Granados, and M. C. Martinez-Bisbal, "Pitfalls to be considered on the metabolomic analysis of biological samples by HR-MAS," Front. Chem. **2**, 33 (2014).
[5]G. Jenkins and C. D. Mansfield, *Microfluidic Diagnostics Methods and Protocols, Methods in Molecular Biology, Methods and Protocols* (Humana Press: Imprint Humana Press, Totowa, New Jersey, 2013), Chap. XIII, 525 p.
[6]A. Bernardi, J. Jimenez-Barbero, A. Casnati, C. De Castro, T. Darbre, F. Fieschi, J. Finne, H. Funken, K. E. Jaeger, M. Lahmann *et al.*, "Multivalent glycoconjugates as anti-pathogenic agents," Chem. Soc. Rev. **42**(11), 4709–4727 (2013).
[7]E. Aznar, R. Martinez-Manez, and F. Sancenon, "Controlled release using mesoporous materials containing gate-like scaffoldings," Expert Opin. Drug Delivery **6**(6), 643–655 (2009).
[8]N. Mas, D. Arcos, L. Polo, E. Aznar, S. Sanchez-Salcedo, F. Sancenon, A. Garcia, M. D. Marcos, A. Baeza, M. Vallet-Regi *et al.*, "Towards the development of smart 3D 'gated scaffolds' for on-command delivery," Small (published online 2014).
[9]S. Jiang, K. Y. Win, S. Liu, C. P. Teng, Y. Zheng, and M. Y. Han, "Surface-functionalized nanoparticles for biosensing and imaging-guided therapeutics," Nanoscale **5**(8), 3127–3148 (2013).
[10]S. Jung, J. Nam, S. Hwang, J. Park, J. Hur, K. Im, N. Park, and S. Kim, "Theragnostic pH-sensitive gold nanoparticles for the selective surface enhanced Raman scattering and photothermal cancer therapy," Anal. Chem. **85**(16), 7674–7681 (2013).
[11]M. P. Melancon, W. Lu, M. Zhong, M. Zhou, G. Liang, A. M. Elliott, J. D. Hazle, J. N. Myers, C. Li, and R. J. Stafford, "Targeted multifunctional gold-based nanoshells for magnetic resonance-guided laser ablation of head and neck cancer," Biomaterials **32**(30), 7600–7608 (2011).
[12]R. A. Murray, Y. Qiu, F. Chiodo, M. Marradi, S. Penades, and S. E. Moya, "A quantitative study of the intracellular dynamics of fluorescently labelled glyco-gold nanoparticles via fluorescence correlation spectroscopy," Small **10**(13), 2602–2610 (2014).
[13]A. P. Candiota, M. Acosta, R. V. Simoes, T. Delgado-Goni, S. Lope-Piedrafita, A. Irure, M. Marradi, O. Bomati-Miguel, N. Miguel-Sancho, I. Abasolo *et al.*, "A new *ex vivo* method to evaluate the performance of candidate MRI contrast agents: A proof-of-concept study," J. Nanobiotechnol. **12**, 12 (2014).
[14]A. van de Stolpe and J. den Toonder, "Workshop meeting report organs-on-chips: Human disease models," Lab Chip **13**(18), 3449-3470 (2013).
[15]J. El-Ali, P. K. Sorger, and K. F. Jensen, "Cells on chips," Nature **442**(7101), 403–411 (2006).
[16]L. Kim, M. D. Vahey, H. Y. Lee, and J. Voldman, "Microfluidic arrays for logarithmically perfused embryonic stem cell culture," Lab Chip **6**(3), 394–406 (2006).
[17]L. Kim, Y. C. Toh, J. Voldman, and H. Yu, "A practical guide to microfluidic perfusion culture of adherent mammalian cells," Lab Chip **7**(6), 681–694 (2007).
[18]A. Tourovskaia, X. Figueroa-Masot, and A. Folch, "Differentiation-on-a-chip: A microfluidic platform for long-term cell culture studies," Lab Chip **5**(1), 14–19 (2005).
[19]E. K. Sackmann, A. L. Fulton, and D. J. Beebe, "The present and future role of microfluidics in biomedical research," Nature **507**(7491), 181–189 (2014).
[20]S. J. Blackband, D. L. Buckley, J. D. Bui, and M. I. Phillips, "NMR microscopy—Beginnings and new directions," Magn. Reson. Mater. Phys., Biol. Med. **9**(3), 112–116 (1999).
[21]M. I. Kettunen and K. M. Brindle, "Apoptosis detection using magnetic resonance imaging and spectroscopy," Prog. Nucl. Magn. Reson. Spectrosc. **47**(3-4), 175–185 (2005).
[22]H. Benveniste and S. J. Blackband, "Translational neuroscience and magnetic-resonance microscopy," Lancet Neurol. **5**(6), 536–544 (2006).
[23]K. Ehrmann, K. Pataky, M. Stettler, F. M. Wurm, J. Brugger, P. A. Besse, and R. Popovic, "NMR spectroscopy and perfusion of mammalian cells using surface microprobes," Lab Chip **7**(3), 381–383 (2007).
[24]T. M. Shepherd, B. Scheffler, M. A. King, G. J. Stanisz, D. A. Steindler, and S. J. Blackband, "MR microscopy of rat hippocampal slice cultures: A novel model for studying cellular processes and chronic perturbations to tissue microstructure," NeuroImage **30**(3), 780–786 (2006).
[25]S. C. Grant, N. R. Aiken, H. D. Plant, S. Gibbs, T. H. Mareci, A. G. Webb, and S. J. Blackband, "NMR spectroscopy of single neurons," Magn. Reson. Med. **44**(1), 19–22 (2000).
[26]S. C. Grant, D. L. Buckley, S. Gibbs, A. G. Webb, and S. J. Blackband, "MR microscopy of multicomponent diffusion in single neurons," Magn. Reson. Med. **46**(6), 1107–1112 (2001).
[27]F. J. Blanco, M. Agirregabiria, J. Garcia, J. Berganzo, M. Tijero, M. T. Arroyo, J. M. Ruano, I. Aramburu, and K. Mayora, "Novel three-dimensional embedded SU-8 microchannels fabricated using a low temperature full wafer adhesive bonding," J. Micromech. Microeng. **14**(7), 1047–1056 (2004).
[28]D. Duval, A. B. Gonzalez-Guerrero, S. Dante, J. Osmond, R. Monge, L. J. Fernandez, K. E. Zinoviev, C. Dominguez, and L. M. Lechuga, "Nanophotonic lab-on-a-chip platforms including novel bimodal interferometers, microfluidics and grating couplers," Lab Chip **12**(11), 1987–1994 (2012).
[29]J. Liu, B. Cai, J. Zhu, G. Ding, X. Zhao, C. Yang, and D. Chen, "Process research of high aspect ratio microstructure using SU-8 resist," Microsyst. Technol. **10**(4), 265–268 (2004).
[30]O. P. Parida and N. Bhat, "Characterization of optical properties of SU-8 and fabrication of optical components," in *ICOP 2009-International Conference on Optics and Photonics, Chandigarh, India*, *30 October–1 November 2009*, edited by CSIO (2009).
[31]A. Altuna, G. Gabriel, L. M. de la Prida, M. Tijero, A. Guimerá, J. Berganzo, R. Salido, R. Villa, and L. J. Fernández, "SU-8-based microneedles for *in vitro* neural applications," J. Micromech. Microeng. **20**(6), 064014 (2010).
[32]L. J. Fernández, A. Altuna, M. Tijero, G. Gabriel, R. Villa, M. J. Rodríguez, M. Batlle, R. Vilares, J. Berganzo, and F. J. Blanco, "Study of functional viability of SU-8-based microneedles for neural applications," J. Micromech. Microeng. **19**(2), 025007 (2009).
[33]M. Ni, W. H. Tong, D. Choudhury, N. A. Rahim, C. Iliescu, and H. Yu, "Cell culture on MEMS platforms: A review," Int. J. Mol. Sci. **10**(12), 5411–5441 (2009).

[34]G. Kotzar, M. Freas, P. Abel, A. Fleischman, S. Roy, C. Zorman, J. M. Moran, and J. Melzak, "Evaluation of MEMS materials of construction for implantable medical devices," Biomaterials **23**(13), 2737–2750 (2002).
[35]K. V. Nemani, K. L. Moodie, J. B. Brennick, A. Su, and B. Gimi, "*In vitro* and *in vivo* evaluation of SU-8 biocompatibility," Mater. Sci. Eng., C **33**(7), 4453–4459 (2013).
[36]L. G. Rigat-Brugarolas, A. Elizalde-Torrent, M. Bernabeu, M. De Niz, L. Martin-Jaular, C. Fernandez-Becerra, A. Homs-Corbera, J. Samitier, and H. A. del Portillo, "A functional microengineered model of the human splenon-on-a-chip," Lab Chip **14**(10), 1715–1724 (2014).
[37]K. Y. Torrejon, D. Pu, M. Bergkvist, J. Danias, S. T. Sharfstein, and Y. Xie, "Recreating a human trabecular meshwork outflow system on microfabricated porous structures," Biotechnol. Bioeng. **110**(12), 3205–3218 (2013).
[38]H. Ahlenius and Z. Kokaia, "Isolation and generation of neurosphere cultures from embryonic and adult mouse brain," Methods Mol. Biol. **633**, 241–252 (2010).
[39]S. Gil-Perotin, M. Duran-Moreno, A. Cebrian-Silla, M. Ramirez, P. Garcia-Belda, and J. M. Garcia-Verdugo, "Adult neural stem cells from the subventricular zone: A review of the neurosphere assay," Anatomical Rec. **296**(9), 1435–1452 (2013).
[40]M. C. Martinez-Bisbal, V. Esteve, B. Martinez-Granados, and B. Celda, "Magnetic resonance microscopy contribution to interpret high-resolution magic angle spinning metabolomic data of human tumor tissue," J. Biomed. Biotechnol. **2011**, 763684.
[41]L. Moroni, J. R. de Wijn, and C. A. van Blitterswijk, "Integrating novel technologies to fabricate smart scaffolds," J. Biomater. Sci., Polym. Ed. **19**(5), 543–572 (2008).